ELSEVIER

Journal of Power Sources 105 (2002) 274–282

JOURNAL OF POWER SOURCES

www.elsevier.com/locate/jpowsour

Recent developments of the measurement of the methanol permeation in a direct methanol fuel cell

H. Dohle*, J. Divisek, J. Mergel, H.F. Oetjen, C. Zingler, D. Stolten

Institute for Materials and Processes in Energy Systems (IWV-3), Energy Process Engineering
Forschungszentrum Jülich GmbH, D-52425 Jülich, Germany

Abstract

The performance and the efficiency of direct methanol fuel cells (DMFCs) are affected by the methanol permeation from the anode to the cathode. A widely used method to measure the methanol permeation in a DMFC is the analysis of the carbon dioxide content of the cathode exhaust. During the operation of a DMFC large amounts of carbon dioxide are produced in the anodic catalyst layer which can diffuse partially to the cathode. As a consequence the carbon dioxide in the cathodic exhaust gas stream is expected to consist of two fractions: the carbon dioxide resulting from the oxidation of the permeating methanol and the carbon dioxide diffusing from the anode to the cathode. In this work we describe a way to separate the distribution of the two fractions under real DMFC operating conditions. As a results we found that with low methanol concentrations (<1 M) and high current densities the amount of carbon dioxide passing from the anode to the cathode can even be higher than the amount of carbon dioxide formed at the cathode by methanol oxidation.

Keywords: DMFC; Fuel cell; Methanol permeation; Mass efficiency; CO_2-diffusion

1. Introduction

Fuel cells are promising energy converters since, due to their operating principle, the efficiency achievable is higher than in power plants or internal combustion engines. The use of methanol as a liquid energy carrier circumvents the difficulties of hydrogen storage. Since in a direct methanol fuel cell (DMFC) the methanol is fed directly, i.e. without the intermediary of a reformer, to the fuel cell, DMFC systems exhibit a particularly simple construction. In a DMFCs, the following catalytically activated reactions take place:

$$\text{for anode}: \quad CH_3OH + H_2O \rightarrow CO_2 + 6H^+ + 6e^-$$

$$\text{for cathode}: \quad 6H^+ + 6e^- + 1.5O_2 \rightarrow 3H_2O$$

$$\text{overall reaction}: \quad CH_3OH + 1.5O_2 \rightarrow CO_2 + 2H_2O$$

Particular problems are posed by methanol permeation through the membrane, which reduces the fraction of useful methanol since the methanol passed to the cathode is converted into carbon dioxide. The formation of a mixed potential at the cathode due to the methanol permeation leads to additional losses the cell voltage is lowered and the electric power decreases.

In addition to the power densities, knowledge of the methanol permeation is therefore of significance for evaluating a DMFCs.

The methanol permeation is converted into a corresponding parasitic electronic current, I_{perm}, using Faraday's law.

$$I_{perm} = \frac{N_{MeOH}^{perm}}{6F} \tag{1}$$

The mass efficiency η_m defines the ratio of the fuel quantity converted for current transformation to the total fuel quantity converted.

$$\eta_m = \frac{I_{el}}{I_{el} + I_{perm}} \tag{2}$$

The DMFC test rig described in the following serves to measure current/voltage curves and for methanol permeation measurement.

2. Experimental facilities

2.1. DMFC test cell

The membrane electrode assembly to be measured is arranged between the anode plate and the cathode plate of the test cell (Fig. 1). The active area of the MEA is 20 cm^2. Electronic contacting of the MEA as well as the

* Corresponding author.

0378-7753/02/$ – see front matter
PII: S0378-7753(01)00953-3

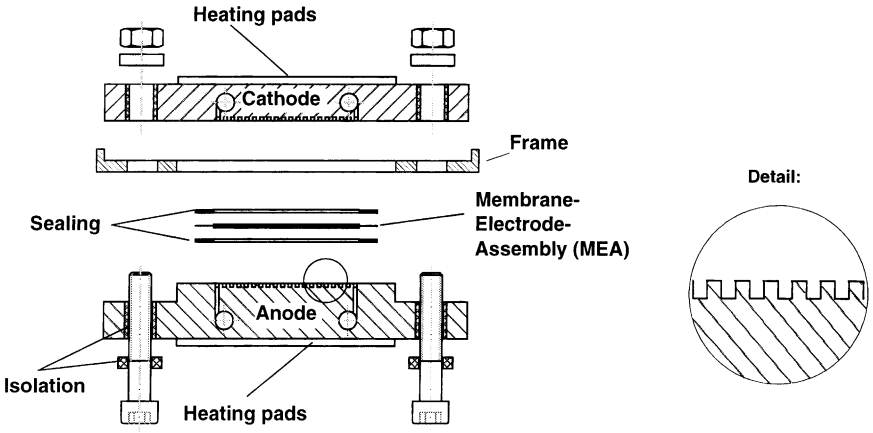

Fig. 1. Schematic diagram of the experimental small-scale DMFC (20 cm^2).

provision of the reaction media is always effected with the aid of a grid structure. The cell plates consist of titanium. The cell has lateral bores for the feed and discharge of the reactants, current tapping and voltage measurement. The current is tapped through plug-in connections. The non-conducting intermediate frame acts on the one hand as an additional electric insulation of anode and cathode and, on the other hand, as a centring aid during installation of the membrane electrode assembly into the test cell. The inactive rim of the MEA along with two PTFE sealings serves for the gas tight separation of the anode and cathode compartments.

In addition, each plate is provided on its rear side with a glued flat heater. Separate heating controllers keep the temperature of the cell at the required value.

2.2. Test rig

2.2.1. Anode side

On the anode side, the test rig consists of a circulation tank, a circulation pump and a condenser serving as a CO_2 separator (Figs. 2 and 3). The preheated methanol/water mixture is taken from the tank through a circulation pump and fed to the cell.

The methanol/water mixture leaves the cell together with the CO_2 produced through the upper cell connection and is passed into the CO_2 condenser supplied with cooling water. The CO_2 is discharged from the system through an upstream pressure controller. The liquid phase flows back into the circulation tank.

In addition, the anode loop can be adjusted to a defined pressure by pressurised nitrogen. The test rig is provided with a device for methanol feed. Depending on the consumption, either pure methanol or a concentrated methanol/water mixture (5 M) is fed into the loop.

2.2.2. Cathode side

On the cathode side, the test rig mainly consists of the gas supply and of components installed behind the cell. The cathode gas required is selected through three-way cocks. Pure oxygen, air and pure nitrogen are available.

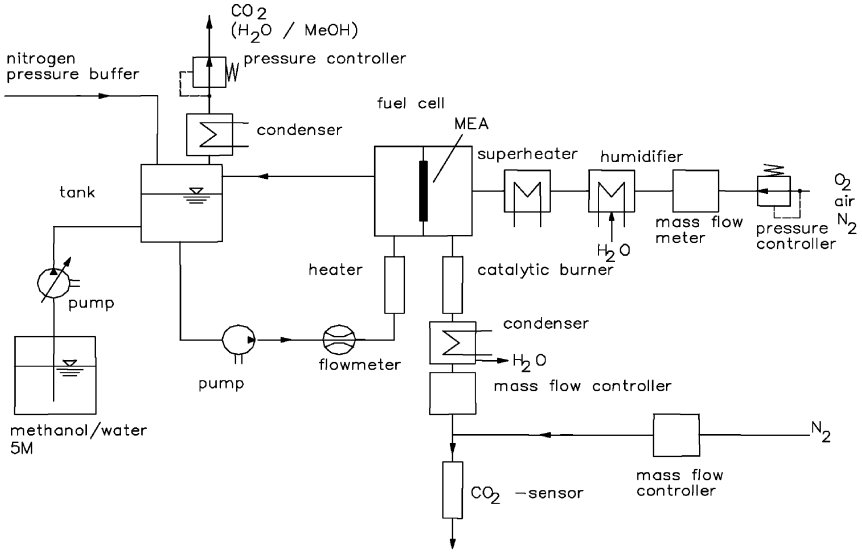

Fig. 2. Schematic diagram of the test rig.

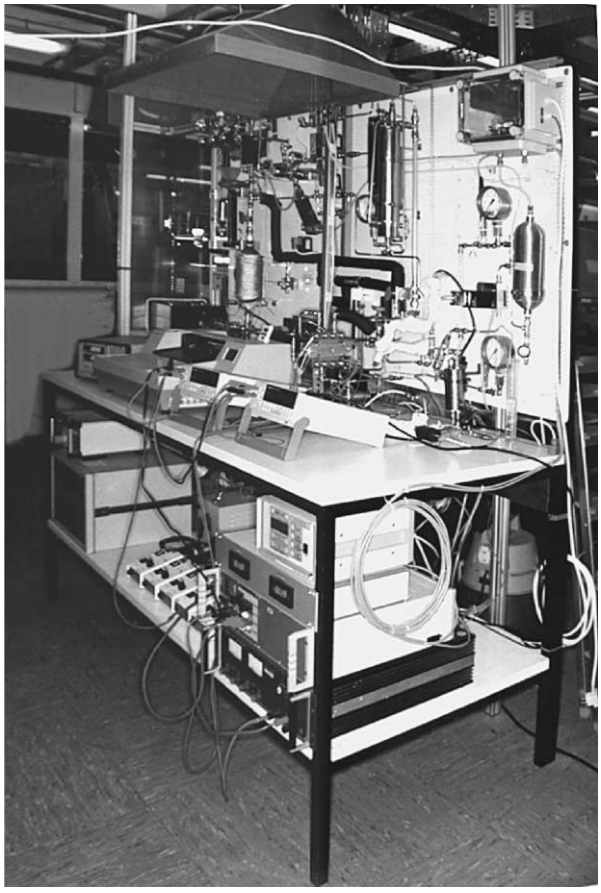

Fig. 3. Test rig for DMFC.

The selected gas is pressurised to the required operating pressure through an upstream pressure controller and fed into the cell through a mass flow meter. The product water and the methanol/water mixture passed from the anode to the cathode is condensed out by a condenser arranged behind the cell. The separated gas phase leaves the condenser through a mass flow controller. Another mass flow controller of the same design mixes this cathode exhaust gas with nitrogen so that the CO_2 partial pressure of the mixture corresponds to the measuring range of the CO_2 sensor (see below).

A heated catalytic afterburner can be switched between cell and condenser, if required. It burns any methanol not converted at the cathode to CO_2 and water. The afterburner consists of a heated tube, which is filled with catalyst material and exhibits a temperature of 230 °C during operation. Pellets of 0.5% Pd on Al_2O_3 are used as the catalyst. A CO_2 sensor (Vaisala GMN 12A) serves for measuring the CO_2 concentration of the cathode exhaust gas.

2.3. Methods

2.3.1. Preparation of the membrane electrode assemblies (MEAs)

The MEAs investigated were prepared in-house by a spraying method. The anode consisted of a carbon cloth support onto which a layer of uncatalysed XC-72 active carbon in an amount of 8 mg/cm^2 bound with 5% PTFE was deposited. The measurements described in this paper were carried out with two different MEAs. The catalyst layer of the first one (MEA1) contained 4 mg/cm^2 of Pt/Ru catalyst (50:50) on carbon and 20% Nafion from a 5% solution with water and low aliphatic alcohols. The cathode was similarly constructed with 4 mg/cm^2 of Pt catalyst on carbon bound with 30% PTFE and an identical uncatalysed layer which served as the backing layer. The MEA was fabricated by hot pressing the two electrodes with a Nafion 117 membrane. The second MEA (MEA2) was fabricated in a similar way. The catalyst loading of MEA2 was only 3 mg/cm^2 on each side and Nafion 112 was used instead of Nafion 117.

2.3.2. Current/voltage curves in oxygen/air operation

For the realisation of current/voltage curves, the test rig is heated to the required temperature and the reactants are adjusted to the desired pressure with the aid of the pressure controllers. No current drain from the cell takes place during heating.

The current/voltage curves are recorded under constant current conditions. The measuring time per point ends when a quasi-steady state is reached, (drift < 10 mV/h) at the latest, however after 1 h.

2.3.3. Half-cell measurements

The half-cell measurements serve to separately evaluate the anode and the cathode. In contrast to the above-described current/voltage curves, the cathode is then under an inert gas atmosphere. The following reactions take place as follows:

$$\text{for anode}: \quad CH_3OH + H_2O \rightarrow CO_2 + 6H^+ + 6e^- \qquad (3)$$

$$\text{for cathode}: \quad 6H^+ + 6e^- \rightarrow 3H_2 \qquad (4)$$

accordingly, the reaction at the anode corresponds to the reaction at the anode under normal working conditions (oxygen/air operation) in the half-cell measurements. In contrast, hydrogen is produced at the cathode (Fig. 4).

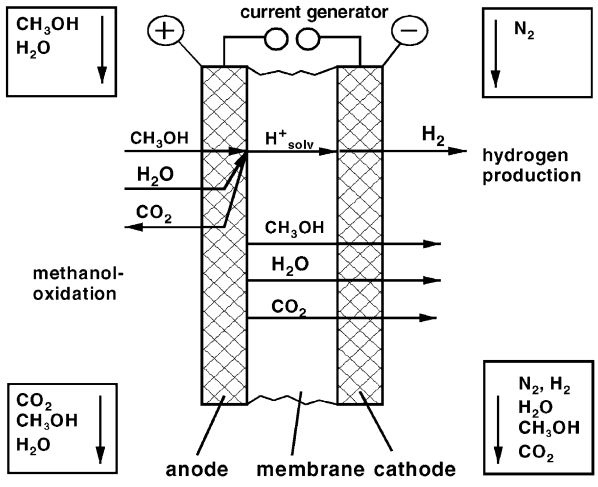

Fig. 4. Half-cell measurement (schematic).

The cathode is thus a reversible hydrogen electrode whose potential is nearly constant in comparison to the anode when passing through the current/voltage curves. Variations in cell voltage are thus essentially attributable to the anode. For reasons of plant safety, nitrogen was used as the carrier gas for the hydrogen produced.

Further methods of half-cell measurement are known from the literature [1]. In these measurements, a reversible hydrogen electrode is arranged as the reference electrode (potential, 0 V) on the anode side at the rim of the membrane electrode assembly so that the potential difference between this electrode and the anode corresponds to the anodic overvoltage. Surampundi et al. perform half-cell measurements at DMFCs varying the catalyst loading and the methanol concentration [2].

2.3.4. Measurement of the methanol permeation

Various measurements for determining the methanol permeation are known from the literature. Lux et al. describe permeation measurements on Nafion without applied electrode [3], whereas Wang et al. determine the methanol permeation in fuel cell operation through mass spectroscopy [4]. The method used in this work is similar to the method described by Valdez and Narayanan [5]. The determination of methanol permeation is effected by a CO_2 sensor. The methanol passed from the anode to the cathode reacts at the cathode and in the subsequent catalytic burner forming CO_2. The total molar flow through the sensor is known from the two mass flow controllers. The CO_2 molar flow results from the CO_2 fraction furnished by the sensor. Hence follows the MeOH molar flow from the stoichiometry of combustion.

$$N_{\mathrm{MeOH}} = N_{\mathrm{CO_2}} = x_{\mathrm{CO_2}} N_{\mathrm{exhaust}} \tag{5}$$

2.4. Measurement of the CO_2 permeation in half-cell operation

In order to determine the methanol permeation through the CO_2 measurement, it is necessary to know the CO_2 fraction passed from the anode to the cathode. This fraction can be approximately determined through half-cell measurements, where CO_2 is only produced at the anode and passed to the cathode. Inert gas (N_2) is present on the cathode side. Methanol is therefore not oxidised on the cathode side.

These measurements take place without a subsequent catalytic burner since otherwise a reforming reaction according to as follows:

$$\mathrm{CH_3OH + H_2O \rightarrow CO_2 + 3H_2} \tag{6}$$

occurs with undesired cathodic CO_2 formation.

In all other respects, the experimental set-up and the evaluation correspond to the method mentioned before; an apparent methanol permeation can be allocated to the CO_2 permeation through the Faraday's law, Eq. (1).

2.4.1. Mass transport mechanisms

As far as the mass transfer of CO_2 from the anode to the cathode is concerned, the mass transfer mechanisms of diffusion and convection come into consideration. In the steady state case, the second-order differential equation

$$D_{\mathrm{CO_2}} \nabla^2 c_{\mathrm{CO_2}} - \nabla(c_{\mathrm{CO_2}} \cdot \vec{v}) = 0 \tag{7}$$

applies to the mass transfer through the membrane, or else the description with $\vec{v}$ as the velocity vector of convection.

$$N_{\mathrm{CO_2}} = D_{\mathrm{CO_2}} \cdot \nabla c_{\mathrm{CO_2}} - c_{\mathrm{CO_2}} \cdot \vec{v} \tag{8}$$

Since the methanol/water mixture is circulated on the anode side, a saturation with carbon dioxide will occur on the anode side after a certain time of operation. The remaining carbon dioxide is discharged from the anode loop. The solubility of the CO_2 is determined by Henry's law. It is fulfilled in good approximation [6] up to CO_2 partial pressures p of 5 bar.

$$c^{\mathrm{an}}_{\mathrm{CO_2}} = p\beta \tag{9}$$

The concentration of methanol in the water is low, so that the data for the solubility of CO_2 in pure water are used in a first estimate. This is done with the following approximation equation (T in °C, $0\,^{\circ}\mathrm{C} < T < 100\,^{\circ}\mathrm{C}$) which has been derived from tabulated data in [6].

$$\beta = 4.208352 \times 10^{-8} T^4 - 1.118743 \times 10^{-5} T^3 + 1.155184 \times 10^{-3} T^2 - 5.9802 \times 10^{-3} T + 1.668656 \left[\frac{\mathrm{cm^3_{CO_2}}}{\mathrm{g_{H_2O}\,bar}}\right] \tag{10}$$

Due to the carrier gas flow on the cathode side and the lack of CO_2 sources in the cathode, the cathodic CO_2 concentration is set equal to zero.

$$c^{\mathrm{cath}}_{\mathrm{CO_2}} = 0 \tag{11}$$

During the operation of the fuel cell, water/methanol mixture reaches the cathode through electro-osmosis. This convective mass transfer is proportional to the ionic current.

$$N^{\mathrm{drag}}_{\mathrm{H_2O+MeOH}} = n_{\mathrm{drag}} \frac{I_{\mathrm{ion}}}{F} \tag{12}$$

The value n_{drag} specifies the number of entrained molecules per proton. In a first approximation no difference is made between water and methanol. The value is temperature-dependent and was measured as follows which is in good agreement with measurements presented in [7] (Table 1).

Table 1
Influence of the temperature on the drag coefficient [8] measured for a methanol/water mixture (methanol concentration 1 M)

Temperature (°C)	n_{drag}
85	4
110	4.3
130	5

3. Measurement of the methanol permeation with CO_2 correction

At the cathode, a CO_2 molar flow is measured during fuel cell operation which is composed, on the one hand, of CO_2 formed due to methanol permeation and, on the other hand, of CO_2 reaching the cathode from the anode.

$$N_{\text{meas}}^{\text{CO}_2} = \frac{I_{\text{perm}}}{6F} + N_{\text{perm}}^{\text{CO}_2} \tag{13}$$

The methanol permeation rate is

$$I_{\text{perm}} = (N_{\text{meas}}^{\text{CO}_2} - N_{\text{perm}}^{\text{CO}_2})6F \tag{14}$$

According to Eq. (8), the molar flux $N_{\text{perm}}^{\text{CO}_2}$ is caused by diffusion and convection:

$$N_{\text{perm}}^{\text{CO}_2} = N_{\text{diff}}^{\text{CO}_2} + N_{\text{conv}}^{\text{CO}_2} \tag{15}$$

The convective flux $N_{\text{conv}}^{\text{CO}_2}$ depends on the current density I, the drag factor n_{drag}, the pressure p and the Henry constant β.

$$N_{\text{conv}}^{\text{CO}_2} = \frac{I}{F} n_{\text{drag}} p \beta M_{\text{W}} \frac{1}{V_{\text{M}}} \tag{16}$$

with $M_{\text{W}} = 18$ g/mol (molecular weight of water) and $V_{\text{M}} = 24{,}412$ cm^3/mol (molar volume).

Compared to the measured values of $N_{\text{perm}}^{\text{CO}_2}$ the convective flux $N_{\text{conv}}^{\text{CO}_2}$ is in the order of only 5–10%. In the following estimation the convective flux is thus considered to be negligible compared to the diffusion flux.

At the anode, the electrochemical conversion of methanol and water takes place at an electronic current I_{el}. In a first approximation, the CO_2 concentration at the anode is set proportional to the electronic current.

$$c_{\text{a}}^{\text{CO}_2} = k_{\text{a}} \frac{I_{\text{el}}}{6F} \tag{17}$$

At the cathode, different processes take place depending on the operating modes.

3.1. Fuel cell operation

The methanol reaching the cathode is oxidised. The permeation rate corresponds to a parasitic current I_{perm}, producing approximately the cathodic CO_2 concentration.

$$c_{\text{k}}^{\text{CO}_2} = k_{\text{k}} \frac{I_{\text{perm}}}{6F} \tag{18}$$

The proportionality factor k_{k} is assumed to be much smaller than the factor k_{a} since PTFE is added as a pore former in the cathodic catalyst layer so that a much lower diffusion resistance than in the anode is to be expected.

$$k_{\text{k}} \ll k_{\text{a}} \quad \text{which leads to} \quad c_{\text{k}}^{\text{CO}_2} \ll c_{\text{a}}^{\text{CO}_2} \tag{19}$$

In addition, CO_2 pressure in the cathode is self-limited by the diffusion of oxygen towards the reactive areas which takes place in the same pore channels as the counter-diffusion of CO_2.

3.2. Half-cell measurement

The methanol reaching the cathode is not converted because of the absence of oxygen. The CO_2 concentration is approximately set equal to zero.

$$\tilde{c}_{\text{k}}^{\text{CO}_2} = 0 \tag{20}$$

3.3. Balance

The CO_2 molar flow passed from the anode to the cathode is assumed to be proportional to the concentration gradient between the anode and the cathode for a width b of the ion-conducting membrane.

$$N_{\text{perm}}^{\text{CO}_2} = -D_{\text{CO}_2}^{\text{mem}} \frac{c_{\text{k}}^{\text{CO}_2} - c_{\text{a}}^{\text{CO}_2}}{b} \quad \text{(fuel cell operation)} \tag{21}$$

$$\tilde{N}_{\text{perm}}^{\text{CO}_2} = -D_{\text{CO}_2}^{\text{mem}} \frac{\tilde{c}_{\text{k}}^{\text{CO}_2} - c_{\text{a}}^{\text{CO}_2}}{b} \quad \text{(half-cell operation)} \tag{22}$$

Assuming $c_{\text{k}}^{\text{CO}_2} \ll c_{\text{a}}^{\text{CO}_2}$ (Eq. (19)) results are as follows:

$$\tilde{N}_{\text{perm}}^{\text{CO}_2} \approx N_{\text{perm}}^{\text{CO}_2} \tag{23}$$

i.e. the CO_2 molar flow from the anode to the cathode in fuel cell operation is similar to the flow in half-cell operation.

In a transformed notation, the actual methanol permeation results are as follows:

$$I_{\text{perm}} = \frac{N_{\text{meas}}^{\text{CO}_2} - \tilde{N}_{\text{perm}}^{\text{CO}_2}}{(1/6F)(1 - (6F\tilde{N}_{\text{perm}}^{\text{CO}_2}/I_{\text{el}})(k_{\text{k}}/k_{\text{a}}))} \tag{24}$$

where the bracketed expression in the denominator has been experimentally determined to be in the range of 0.9–0.95. In a first approximation, the measurement of the methanol permeation can thus be estimated from the measurements of the CO_2 content of the cathode exhaust gas in fuel cell and in half-cell operation.

$$I_{\text{perm}} \approx 6F(N_{\text{meas}}^{\text{CO}_2} - \tilde{N}_{\text{perm}}^{\text{CO}_2}) \tag{25}$$

4. Experimental results

4.1. Testing of the catalytic burner

Due to the large amounts of oxygen ($\lambda > 10$) one should expect complete heterogeneous catalysis at the cathode and full conversion of the permeated methanol to carbon dioxide within the cell. The measurements were carried out on a GC–MS (Hewlett-Packard HP6890, HP5973) using a HPPLOT-Q column of 30 m length and 0.2 mm diameter. Carrier gas was helium with a flow rate of 1.6 ml/min. As a result we found in the cathode exhaust gas stream noticeable traces of organic compounds such as methanol or methylformate (Fig. 5, top). By the use of the catalytic burner after the cathode gas exhaust the organic compounds could be

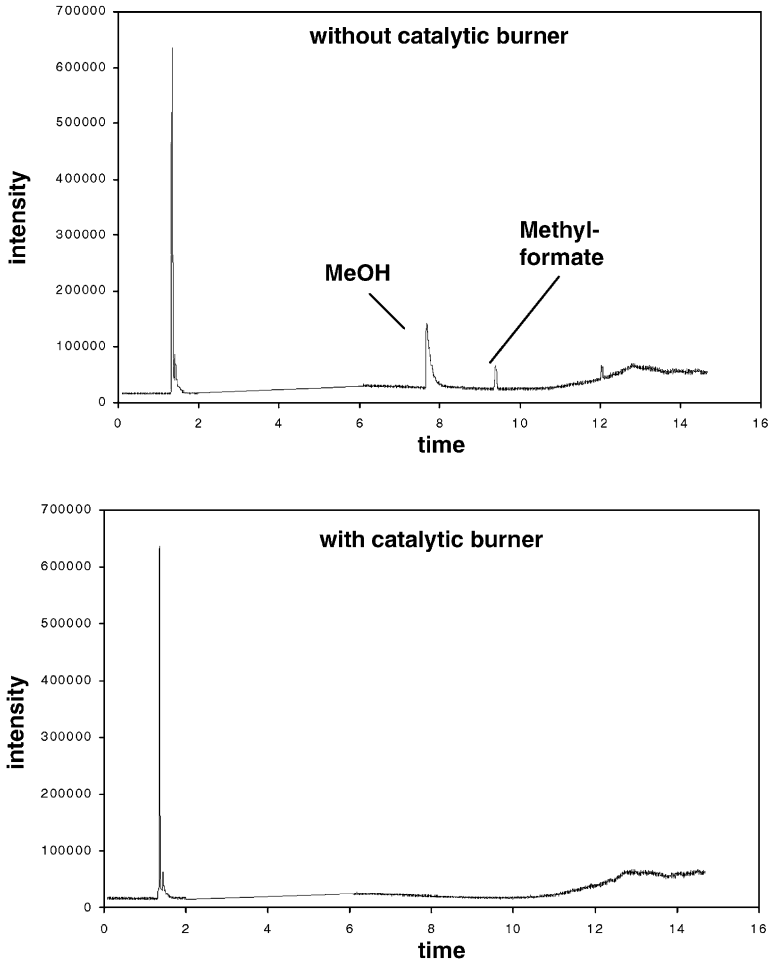

Fig. 5. Qualitative GC–MS measurement of the cathodic exhaust gas stream of a direct methanol fuel cell with and without catalytic burner (see Fig. 2). The peaks in the output signals indicate the presence of at least methanol and methylformate in the cathodic cell exhaust (top), which are converted in the catalytic burner (bottom) to carbon dioxide. The first peak in each diagram is caused by air, peaks which belong to water have been removed.

converted into carbon dioxide, so that the peaks in the GC–MS signal disappeared (Fig. 5, bottom).

A possible explanation is the presence of high amounts of water in the pores of both the catalyst layer and the diffusion layer (cathode side) lowering the oxygen-diffusion towards the reactive areas and enabling the methanol to pass through the catalyst layer without getting in contact with both oxygen and catalyst particles.

4.2. Measurement of the CO_2-diffusion

Experiments were carried out under different operating conditions to determine the CO_2-diffusion from the anode to the cathode. The parameters varied were the temperature of the cell, the pressures on the anode and on the cathode side as well as the anodic methanol concentration. A further parameter was the volume flow of the cathodic inert gas.

4.2.1. Effect of methanol concentration

A change in methanol concentration leads to a modification of the CO_2 permeation from the anode to the cathode. During the operation of the fuel cell, carbon dioxide is formed in the anodic catalyst layer, which in part reaches the cathode through the membrane. Fig. 6 shows the CO_2 permeation for different methanol concentrations plotted over the current density. The CO_2-diffusion is plotted in the (mol/cm^2 s) unit and, on the other hand, an apparent methanol permeation is assigned to the CO_2-diffusion flow according to Eq. (26).

$$N_{CO_2}^{diff} = \frac{I_{eq}^{perm}}{6F} \tag{26}$$

At low current densities the CO_2 molar flows first rise independent of the methanol concentration. The smallest methanol concentration of 0.5 M leads to a plateau formation with increasing current intensity since the CO_2 permeation does not increase any further. The reason is a movement of the reaction zone away from the catalyst layer/membrane phase boundary towards the anodic gas diffuser with rising current density due to diffusion overvoltages of the methanol in the catalyst layer. With an increase of the methanol concentration no plateau formation occurs any more since the displacement of the reaction zone is less pronounced.

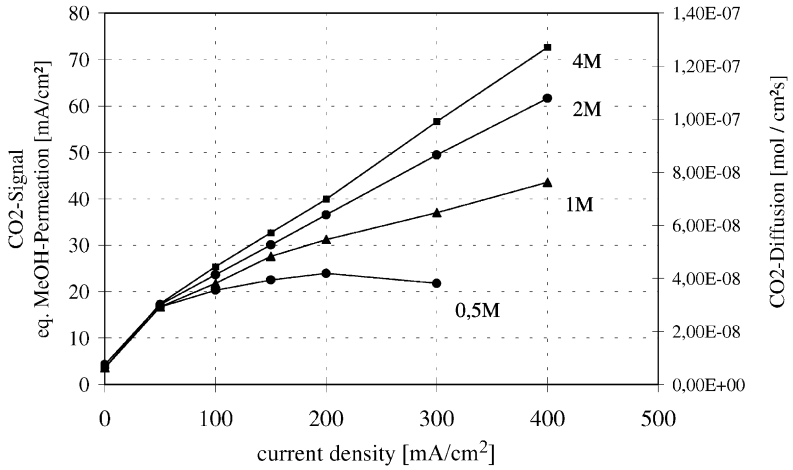

Fig. 6. Influence of the methanol concentration on the CO_2 permeation.

In the zero-current state the diffusion rates are low, although on the anode side a CO_2-saturated methanol/water mixture is present. In the zero-current state no CO_2 is formed inside the catalyst layer on the anode side. Consequently, CO_2 must diffuse from the methanol/water mixture not only through the membrane, but also through the current collector, the diffusion layers and also through the catalyst layer. The effects of the methanol concentration on the CO_2 have been also investigated by modelling calculations. The model has been presented elsewhere [9].

4.2.1.1. Anodic overvoltage. The displacement of the reaction zone is accompanied by an increase of the anode potential due to diffusion overvoltages.

The behaviour of the anode for a change of the methanol concentration is shown in Fig. 7. In the current density range below 100 mA/cm^2, the polarisation curves are on top of each other so that diffusion effects do not have any influence on the overvoltages. At the smallest methanol concentration considered (0.5 M), a limiting current is beginning to form at a current density of 300 mA/cm^2. Higher methanol concentrations lead to lower overvoltages. For the methanol concentration of 1 M, anodic and cathodic pressure variations are additionally carried out in order to evaluate the influence of pressure on the anodic overvoltage. It is apparent that the anode pressure only has insignificant effects on the anode potential.

4.2.2. Effect of pressure and temperature

Figs. 8 and 9 show the influence of pressure changes on the measured CO_2 permeation. A change of the anode pressure leads to a change of the CO_2 permeation of the

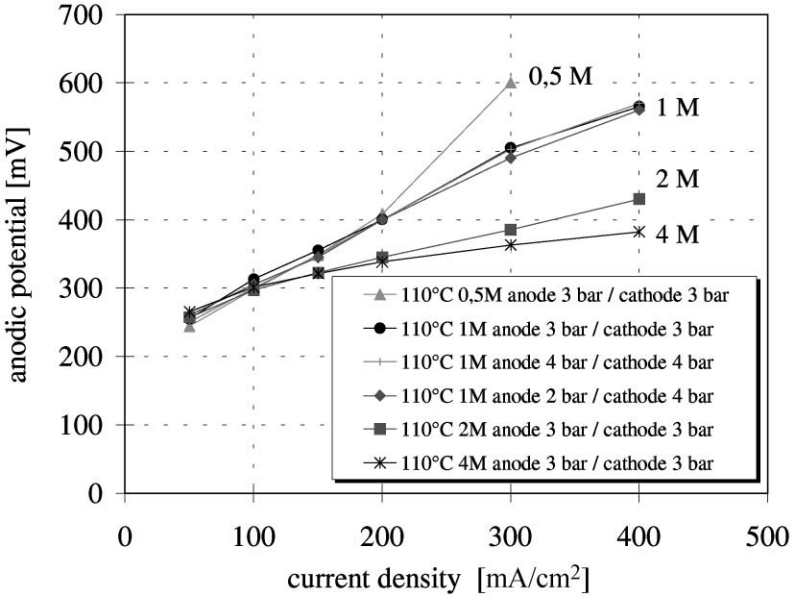

Fig. 7. Influence of the methanol concentration on the anode potential of the DMFC (measurement). Anode activity was measured vs. an H_2 evolving cathode. The amount of catalyst was 4 mg/cm^2 PtRu with 60%C on the anode and 4 mg Pt at the cathode.

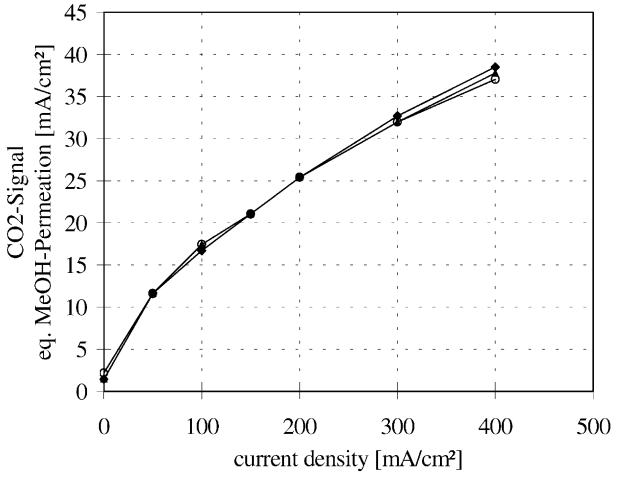

Fig. 8. Influence of the cathode pressure on the CO_2-diffusion in a DMFC: (◆), 2 bar; (▲), 3 bar; (○), 4 bar.

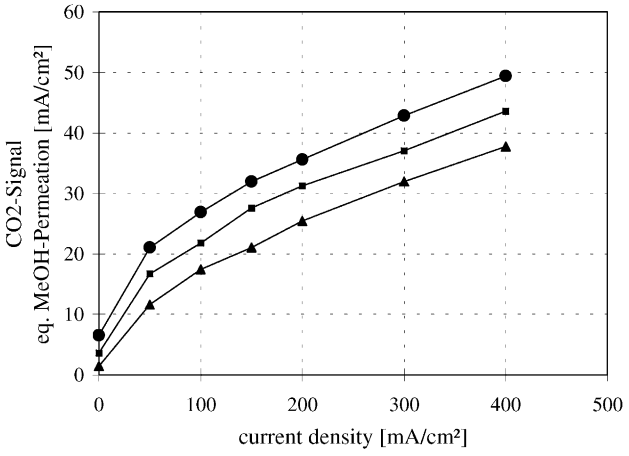

Fig. 9. Influence of the anodic pressure on the CO_2-diffusion in a DMFC: (▲), 2 bar; (■), 3 bar; (●), 4 bar.

order of 6 mA/cm^2 bar, whereas the effects are negligible for changes of the cathode pressure. This is due to the fact that according to Henry's law Eq. (9) the dissolved quantity of CO_2 is proportional to the pressure.

The influence of the temperature is shown in Fig. 10. An increase in temperature results in a decrease of the CO_2 permeation. This is due to the decreasing solubility of CO_2 according to Eq. (10).

4.2.3. Effect of membrane thickness

In the following, the influence of the membrane thickness on the CO_2 permeation will be investigated (Figs. 11 and 12). The lower dotted curves represent the CO_2 permeation in Nafion 117 (175 μm) and in Nafion 112 (50 μm) measured in half-cell operation. Qualitatively, the ratio of these curves corresponds to the reciprocal value of the thickness ratios.

A methanol permeation measurement with a membrane electrode assembly with Nafion 117 (175 μm) is shown in

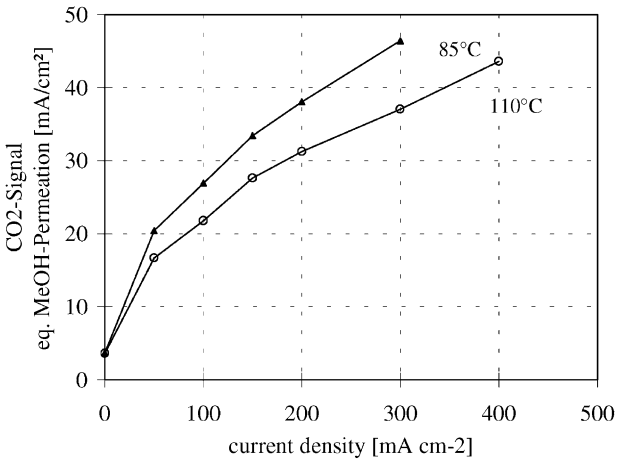

Fig. 10. Influence of the temperature on CO_2-diffusion in a DMFC.

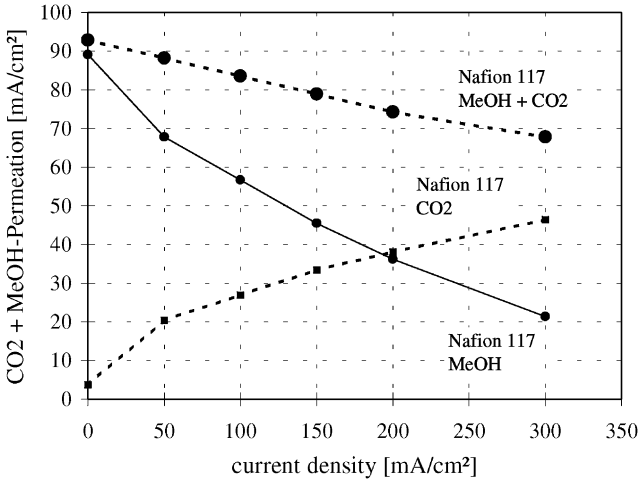

Fig. 11. Methanol permeation rate of a MEA with Nafion 117. Anode loading: 4 mg/cm^2 PtRu; cathode loading 4 mg/cm^2 Pt (85 °C, 1 M, O_2 3 bar).

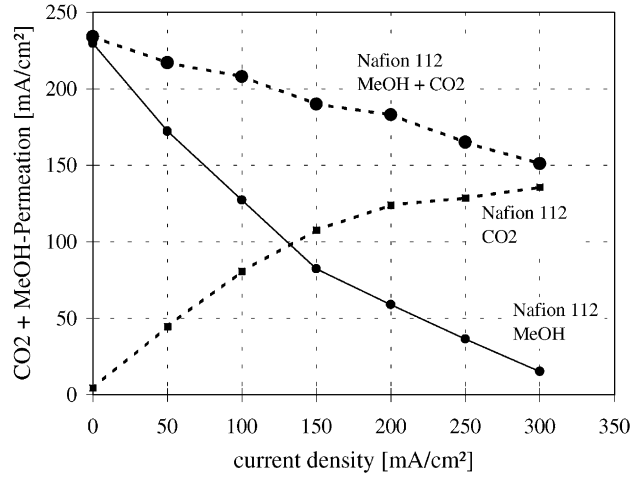

Fig. 12. Methanol permeation rate of a MEA with Nafion 112. The anode consists of 3 mg/cm^2 PtRu with 60% C, the cathode consists of 3 mg/cm^2 (operating conditions: 90 °C; 1 M MeOH; O_2 2.5 bar).

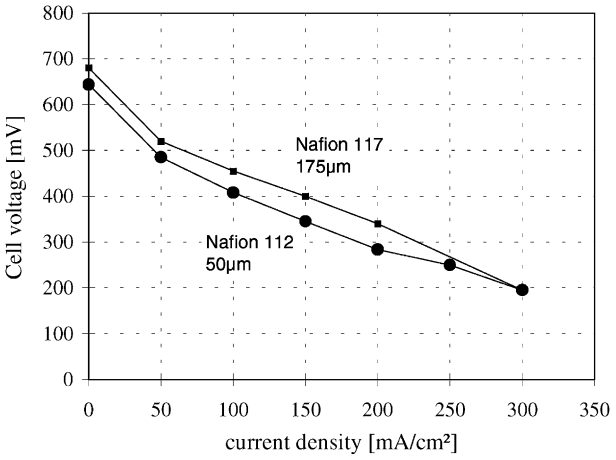

Fig. 13. Influence of the membrane thickness on the current/voltage curve of a DMFC.

Fig. 11. Three different curves are plotted: (1) the measured signal in fuel cell operation; (2) the measurement of the CO_2 signal in half-cell measurement (hydrogen production); and (3) the corrected measurement of methanol permeation. It can be seen that the corrected measurement curve is clearly lower towards high current densities than the uncorrected one. At a concentration of 1 M the methanol concentration inside the catalyst layer decreases due to methanol consumption with flowing current. At a current density of 300 mA/cm^2 an actual methanol permeation rate of approximately 20 mA/cm^2 is to be expected if the anodic CO_2 formation is taken into account.

The permeation curves of a MEA with Nafion 112 (50 µm) in Fig. 12 show a significantly higher methanol diffusion rate (240 mA/cm^2) at no load in comparison to a MEA with Nafion 117 (90 mA/cm^2). This is solely due to the different membrane thicknesses. An essential feature is the steep descent of the CO_2-corrected permeation curve, which leads to a similar methanol permeation rate in the high current density range at approximately 300 mA/cm^2. Fig. 13 finally shows as a trend the effect of methanol permeation in MEAs with different membrane thicknesses. However, the curves are not exactly comparable since a slightly lower catalyst loading was used for the thinner membrane. The MEA with Nafion 117 has 4 mg/cm^2 on each side, the MEA with Nafion 112 only 3 mg/cm^2. At no load, the open-circuit voltage is lower when using Nafion 112 due to the higher methanol permeation rate. Methanol permeation decreases with increasing current density, thus reducing the effects of mixed potential formation. At a current density of approximately 200 mA/cm^2 the lower curve (MEA with Nafion 112) clearly begins to move towards the upper curve. At 300 mA/cm^2 both curves exhibit the same cell voltage.

5. Conclusion

As a result we found that with low methanol concentrations (1 M) and high current densities the amount of carbon dioxide passing from the anode to the cathode can even be higher than the amount of carbon dioxide formed at the cathode by methanol oxidation. The actual methanol permeation rates are thus much lower than expected. As a consequence it is possible to obtain a high mass efficiency at high power densities even with thin membranes.

This property has consequences for the design and operation of DFMCs. The use of thinner membranes more permeable for methanol makes higher demands on the control of the methanol concentration, but probably has advantages with respect to the internal resistance and thus to the overall efficiency. If the methanol concentration exceeds the optimum at a given current density, an excessively high methanol concentration is established at the interface between anodic catalyst layer and membrane. The lower the diffusion resistance of the membrane, the higher will then be the actual methanol permeation.

Irrespective of the thickness of the membrane used, a methanol concentration which is too low will lead to anodic overvoltages with negative effects on the power density and efficiency. Thus, the overall efficency of a DMFCs strongly depends on the regulation of an optimised methanol concentration.

Acknowledgements

We would like to thank Dr. C. Palm (IWV-3) for the GC–MS-analysis.

References

[1] A. Küver, I. Vogel, W. Vielstich, J. Power Sources 52 (1994) 77.
[2] S. Surampundi, S.R. Narayanan, E. Vamos, H. Frank, G. Halpert, A. LaConti, J. Kosek, G.K. Surya Prakash, G.A. Olah, J. Power Sources 47 (1994) 377.
[3] K.W. Lux, J.S. Wainright, R.F. Savinell, U. Landau, in: Proceedings of the Symposium on Electrode Materials and Processes for Energy Conversion and Storage, Electrochemical Society, Vol. 94–23, San Francisco, California, 1994, pp. 302–314.
[4] J.-T. Wang, S. Wasmus, R.F. Savinell, J. Electrochem. Soc. 143 (1996) 1233.
[5] T.I., Valdez, S.R. Narayanan, in: Proceedings of the 2nd International Symposium on Proton Conducting Membrane Fuel Cells II, Electrochemical Society, Vol. 98-27, Pennington, New Jersey, 1998, pp. 380–387.
[6] E. Landolt-Börnstein, Vol. II, Springer, Berlin, 1962.
[7] X. Ren, W. Henderson, S. Gottesfeld, J. Electrochem. Soc. 144 (1997) 267.
[8] H. Dohle, Ph.D. Thesis, RWTH Aachen, 2000.
[9] H. Dohle, J. Divisek, R. Jung, J. Power Sources 86 (2000) 469.